Biosensors and Bioelectronics 123 (2019) 178–184

Contents lists available at ScienceDirect

Biosensors and Bioelectronics

journal homepage: www.elsevier.com/locate/bios

Flexible freestanding graphene paper-based potentiometric enzymatic aptasensor for ultrasensitive wireless detection of kanamycin

Yao Yao, Chengmei Jiang, Jianfeng Ping*

School of Biosystems Engineering and Food Science, Zhejiang University, 866 Yuhangtang Road, Hangzhou 310058, PR China

ARTICLE INFO

Keywords:
Potentiometric aptasensor
Graphene paper
Kanamycin
Flexible sensor
Smartphone

ABSTRACT

Flexible sensing devices have drawn tremendous attention in the past decades due to their potential applications in future hand-held, potable consumer, and wearable electronics. Here, we firstly developed an ultrasensitive wireless potentiometric aptasensor based on flexible freestanding graphene paper for kanamycin detection. Flexible graphene paper made from a simple vacuum filtration method was used as a biocompatible platform for effective immobilization of aptamer. A nuclease-assisted amplification strategy was introduced into this potentiometric biosensing system in order to significantly improve the detection sensitivity through a classic catalytic recycling reaction of target induced by the nuclease (DNase I). As expected, an ultra-low detection limit of 30.0 fg/mL for kanamycin was achieved. Furthermore, the developed potentiometric enzymatic aptasensor exhibits high selectivity, favorable flexibility, excellent stability and reproducibility, which holds great promising for its routine sensing application.

1. Introduction

Kanamycin, an aminoglycoside antibiotic, which is purified from the fermentation of Streptomyces Kanamyceticus (Bai et al., 2014; Spahn and Prescott, 1996). It is commonly used as a veterinary medicine in animal husbandry, aquaculture, and agriculture, a variety of infections could be avoided by the kanamycin-induced genetic mistranslation and restraining translocation indirectly in the protein synthesis (Song et al., 2011; Wirmer and Westhof, 2006). By this reason, kanamycin was overused which results in the existing of its residue in agricultural products and environment (Song et al., 2011). However, huge risk to human health could be caused with the long-term consumption of kanamycin residues, such as hearing loss and toxicity to the kidney (Prosen et al., 1978; Tachibana et al., 1976). Therefore, the development of highly sensitive, accurate, cost-effective, and robust methods for kanamycin determination is in high demand for food safety. Up to now, various determination methods have been developed for the kanamycin detection. The conventional detection methods, including enzyme-linked immunosorbent assay method (ELISA) (Gaudin et al., 2003; Samsonova et al., 2005), high-performance liquid chromatography (HPLC) (Blanchaert et al., 2013; Chen et al., 2006; Manyanga et al., 2010), and high-performance capillary electrophoresis (HPCE) (Kaale et al., 2001; Yu et al., 2009), always require time-consuming sample pretreatment, expensive equipment, and highly skilled operators. And the other methods like colorimetry (Xu et al., 2015) and fluorescence (Chen et al., 2015) are more complex, with a relatively higher detection limit and narrower detection range (Lan et al., 2017). Therefore, the determination of kanamycin with high sensitive, inexpensive, and easy operation is still a challenge.

Electrochemical detection techniques possess a series of advantages, such as excellent sensitivity and controllability, rapid response, and inexpensive (Hu and Xu, 2010; Sentic et al., 2015), which have been recognized as one of the most reliable analytical methods for rapidly detecting (bio)chemical species in environmental, food, and biological samples. Among them, the potentiometry could be counted as the simplest, most portable, and widespread method among the various electrochemical techniques. Particularly, the development of all-solid-state potentiometric sensors have significantly promote the application of potentiometry in analytical field, since they have hugely improved the detection limit, simplified the sensing device construction, and more importantly, which could be assembled into miniaturized devices (Bakker and Pretsch, 2007). Recently, flexible electrode substrates, as a new development tendency of potentiometry (Chem, 2012; Ping et al., 2013), show great superiority in the mechanical performance, fabrication cost, and integration of the developed sensors, which holds great promising in the development of next-generation potentiometric sensing equipment.

Recently, freestanding paper-like flexible electrodes have obtained

---

* Corresponding author.
E-mail address: jfping@zju.edu.cn (J. Ping).

https://doi.org/10.1016/j.bios.2018.08.048
Received 21 June 2018; Received in revised form 20 August 2018; Accepted 21 August 2018

considerable attention due to their tremendous potential in the application of adhesive layers, protective layers, chemical filters, as well as wearable sensing and energy devices (Gwon et al., 2011; Park et al., 2010; Pitkethly, 2004; Wan et al., 2017). Many nanoscale species have been successfully applied to fabricate freestanding paper-like materials with desired structures and outstanding properties to satisfy the increasing requirements of various specific applications (Acerce et al., 2017; Ballard and Rideal, 1983; Cong et al., 2013; Zhang et al., 2013). Among them, the freestanding graphene paper (GNP), exhibits distinct advantages of simple synthesis processes, comparable mechanical properties, excellent electrical conductivity, and satisfactory biological performance, has shown huge potential in the development of various electrochemical sensors, including potentiometric sensors, amperometric sensors, and voltammetric sensors (Ping et al., 2013; Xiao et al., 2012; Yao and Ping, 2018; Zan et al., 2016). Most importantly, benefiting from the easy functionalization and integrating of graphene (Ping et al., 2011, 2015), the specific detection using GNP-based sensors could be easily realized by modifying with various recognition elements (such as antibody, peptide) through covalent or non-covalent bonding (Guo et al., 2012; Wang et al., 2013). In addition, aptamer exhibits excellent stability, wide applicability and great specificity superior to antibodies (Liu et al., 2009; Mayer, 2010; Willner and Zayats, 2007), has been recognized as promising molecular receptors in biosensing applications (Tuerk and Gold, 1990; Ellington and Szostak, 1992). However, GNP modified with aptamer for the construction of flexible potentiometric aptasensor has not been reported yet.

In this study, for the first time, we fabricated a flexible and convenient potentiometric enzymatic aptasensor based on the freestanding GNP for ultrasensitive wireless detection of kanamycin. Freestanding GNP was fabricated through a simple vacuum filtration method, which could be used as a biocompatible platform for effective immobilization of aptamers via π-π stacking interaction. To overcome the limitation of the signal response and sensitivity induced by the 1:1 binding strategy that each aptamer binds to only one single target molecule, we applied a convenient catalytic recycling strategy based on the adoption of DNase I (Scheme 1). Based on this strategy, we established a DNase I-assisted amplification method for ultrasensitive detection of kanamycin on freestanding GNP-based potentiometric biosensing platform. The real-time measurement was recorded on a smartphone wirelessly connected to the potentiometric sensor, which significantly simplifies the design and reduces the cost of detection system. In addition, the determination of kanamycin in milk sample was applied to prove the feasibility of the prepared potentiometric enzymatic aptasensor for real application.

2. Experimental

2.1. Materials and reagents

Kanamycin sulfate, ciprofloxacin hydrochloride monohydrate (purity ≥ 98%), and deoxyribonuclease I (DNase I) were purchased from Sigma-Aldrich (St. Louis, MO, USA). Tetracycline hydrochloride and amoxicillin (purity ≥ 98%) were purchased from Aladdin Chemistry Co., Ltd. (Shanghai, China). Chloramphenicol and graphite were purchased from Alfa Aesar Co., Ltd. (Shanghai, China). Tris-buffer solution (20 mM Tris-HCl, 100 mM NaCl, 5 mM KCl, 2 mM $MgCl_2$, and 1 mM $CaCl_2$, pH 7.4) was used as buffer solution. The kanamycin aptamer with a sequence of 5′-AGATGGGGGTTGAGGCTAAGCCGA-3′ was synthesized by Shanghai Sangon Biotechnology Co., Ltd. (Shanghai, China), which could bind with kanamycin molecule specifically (Guo et al., 2015). All other analytical grade reagents and ultrapure water were used in the experiments.

2.2. Apparatus

The potentiometry tests were conducted with a portable PalmSens instrument (Palm Instrument BV, Houten) which connects to a smartphone by means of an embedded wireless bluetooth module. The smartphone (model Samsung Galaxy SIII) was of Samsung India Limited make. Electrochemical experiments of cyclic voltammetry (CV) were performed on a CHI 760E electrochemical workstation (Chenhua Instruments Co., Shanghai, China). The scanning electron microscope (SEM) was carried out on a SU8010 field emission scanning electron microscope (Hitachi, Japan). Raman spectra were obtained on a micro-Raman spectrometer excited by 514 nm laser excitation (Jobin Yvon LabRam HRUV, France). Electrochemical impedance spectroscopy (EIS) experiment was carried out on a Solartron Analytical model 1260 Impedance-Gain-Phase Analyzer incorporated with a model 1287 Electrochemical Interface (Solartron Analytical, Farnborough, UK), and the experiment was supported by the Zview and Zplot software.

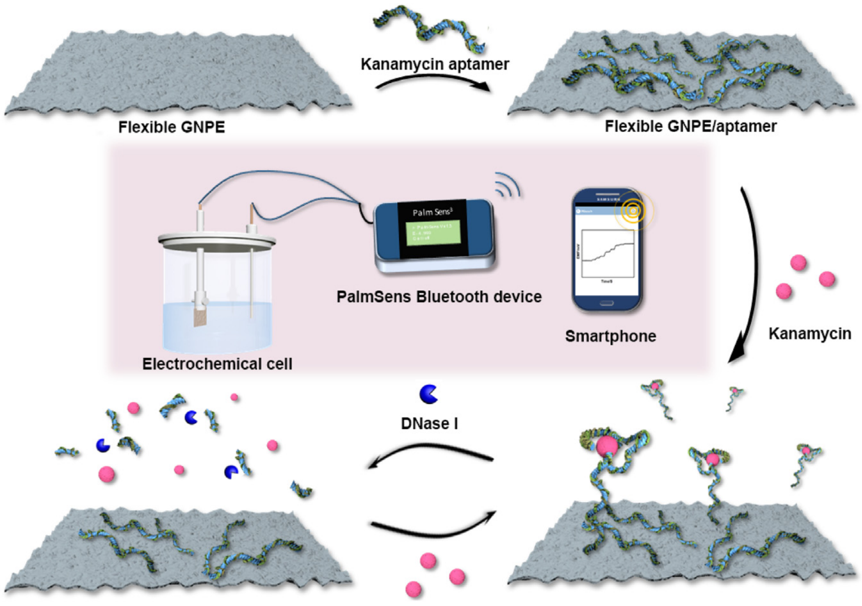

Scheme 1. Schematic illustration of the principle of flexible freestanding GNP-based potentiometric enzymatic aptasensor for nuclease-based amplification detection of kanamycin.

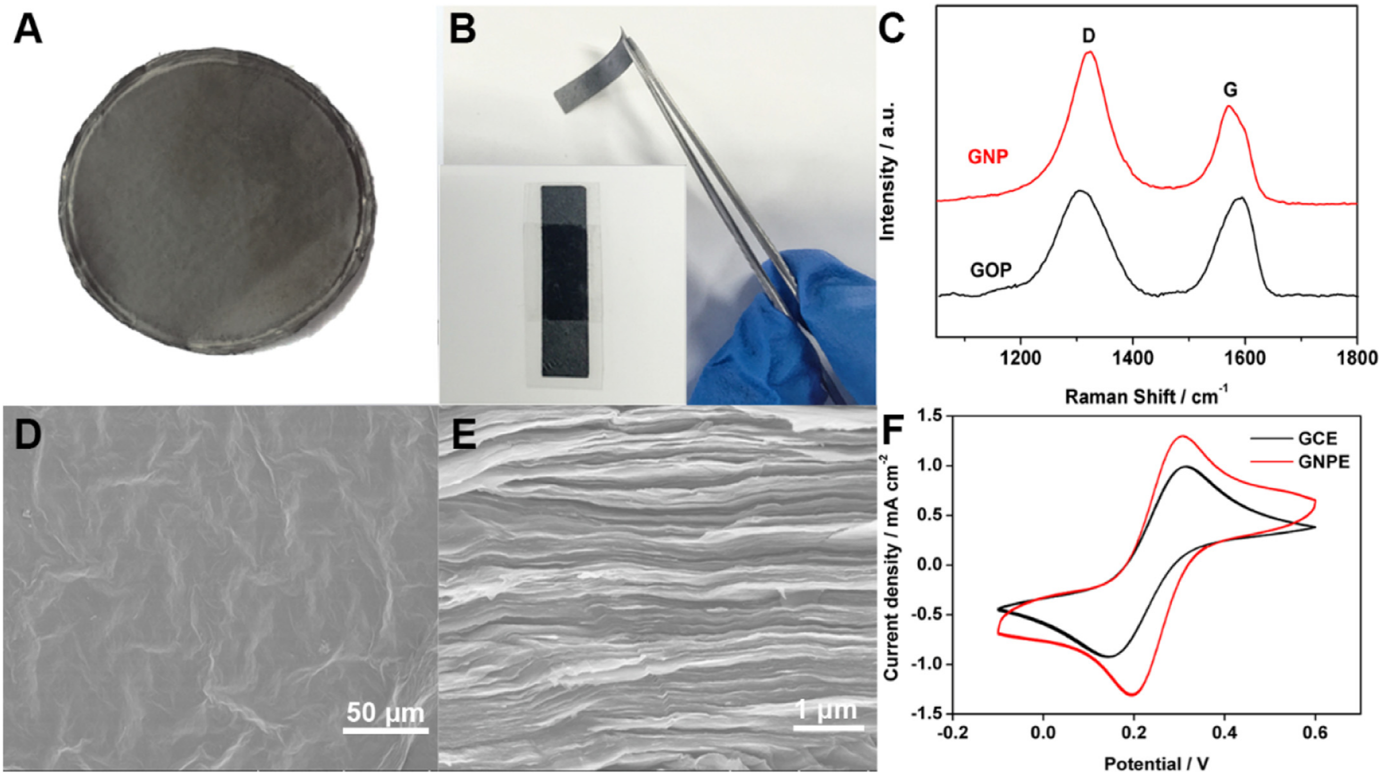

Fig. 1. Characterization of freestanding GNP. (A, B) Digital camera images of GNP (A) and GNP strip (B). (C) Raman spectra of GNP and GOP. (D, E) SEM images of plan views (D) and cross-sectional views (E) of GNP. (F) Cyclic voltammetry of GNPE and GCE in 0.1 M KCl aqueous solution containing 5.0 mM $K_3[Fe(CN)_6]/K_4[Fe(CN)_6]$ (1:1). Scan rate is 100 mV s^{-1}.

2.3. Preparation of potentiometric biosensor

A modified Hummers method (Jr and Offeman, 1958; Kovtyukhova et al., 1999) was used to prepare the suspension of graphite oxide. Homogeneous graphene oxide (GO) dispersion was obtained from graphite oxide suspension (1.0 wt%) through an ultrasonic treatment with ice-water bath. A chemical reduction method based on ascorbic acid as reducing agent was used to convert GO into graphene (Zhang et al., 2010). GNP was fabricated by vacuum filtration of the reduced GO aqueous solution via a nitrocellulose membrane (Sartorius Stedim), in which the pore size is 0.2 μm and the diameter is 47 mm. The obtained GNP could be easily peeled off the nitrocellulose membrane after air-drying at room temperature. And a GO paper (GOP) could be fabricated directly from the GO suspension using the same procedure.

In order to prepare the potentiometric sensing electrode, rectangular GNP strips with a size of 5 mm × 20 mm were firstly obtained from the fresh-prepared GNP. Two plastic masks then stick to both sides of GNP strip (Fig. 1). A GNP electrode (GNPE) with a sensing part size of 5 mm × 5 mm and an electrical conducting area of 5 mm × 5 mm at both ends of GNP strips were obtained. After this step, the GNPE/aptamer was properly fabricated by immersing the GNPE into 500 μL of kanamycin aptamer solution (5 μM) dispersed in 20 mM Tris-buffer solution (pH 7.4) overnight and washed with deionized water gently before use. The aptamer binds with GNPE through non-covalent physical absorption.

For impedance measurement, the experiment was carried out in 0.1 M KCl solution containing 5.0 mM $K_3[Fe(CN)_6]/K_4[Fe(CN)_6]$ (1:1). For the characterization of kanamycin detection, the electrode (denoted as GNPE/aptamer + kanamycin) was prepared by incubating the GNPE/aptamer in Tris-buffer solution with a kanamycin concentration of 120 ng/mL for 30 min. To characterize the enzyme-assisted amplification, the electrode (denoted as GNPE/aptamer + kanamycin + DNase I) was obtained by immersing the GNPE/aptamer in Tris-buffer solution (30 min) with a kanamycin concentration of 120 ng/mL and 10 unit of DNase I which incubated at 37 °C for 30 min beforehand. All the prepared electrodes were washed by distilled water thoroughly and dried at room temperature before use.

2.4. Potentiometric detection

Potentiometric detection was performed by real-time measurement of the electro motive force (EMF) between the terminals of a two-electrode system consisting of the GNPE/aptamer as the working electrode, and a saturated commercial Ag/AgCl electrode (3.3 M KCl solution) as the reference electrode in a detection cell under the constant stirring conditions, the electrolyte used in the cell was 20 mM Tris-buffer solution (pH 7.4). The EMF value was recorded synchronously in our own smartphone based on the android application (app) provided by the company. For the detection of kanamycin, DNase I was firstly incubated at 37 °C for 30 min, then 10 unit of DNase I was added to the detection cell. After the EMF value of GNPE/aptamer-based sensor reached a steady condition, a range of kanamycin concentrations, 0.02–120 pg/mL, were added in the detection cell (10 mL). All the potentiometric tests were operated at room temperature (25 ± 1 °C).

2.5. Real application in milk samples

The application of GNPE/aptamer-based potentiometric aptasensor for kanamycin detection in milk samples worked as follows, five kanamycin-free milk samples purchased from a local supermarket (Hangzhou, China) were added with quantitatively standard kanamycin solution used as artificially contaminated milk samples. Briefly, 20 mL of raw milk was diluted with 20 mL of Tris-buffer solution (pH 7.4, 20 mM), then pH of the sample solution was adjusted to 4.6 by dropwise adding acetic acid (20%, υ/υ) to denaturalize and precipitate the proteins in milk at the isoelectric point. Subsequently, the sample was water bathed at 45 °C for 10 min to ensure the protein precipitated thoroughly. Then, the sample was centrifuged at 10,000 rpm for 30 min, the precipitation was removed and then the sample was filtered with a 0.22 μm membrane. Finally, the pH of the sample was adjusted to 7.4 and a certain amount of kanamycin was added into the pretreated milk sample, then the potentiometric detection of kanamycin was carried out.

3. Results and discussion

3.1. Mechanism of the potentiometric aptasensor

As illustrated systematically in Scheme 1, the potentiometric aptasensor composed by a GNPE/aptamer and a reference electrode, the aptamer is initially bonded to the bare GNPE surface via π-π stacking and hydrophobic interactions between the nucleobases and graphene to avoid the cleavage effect of DNase I (Varghese et al., 2010). Once the kanamycin molecule is introduced into the solution, the aptamer specifically binds with the target to forms a stable, rigid structure and consequently desorbs from the GNPE surface via overcoming the strong π–π interactions, simultaneously tends to separate its negatively ionized phosphodiester groups at a pH value of 7.4 (Hernández et al., 2014; Zelada-Guillén et al., 2009). Since the GNPE act as asymmetric capacitors, this variation of charges provokes a subsequent change of the recorded potential values. And the un-immobilized nuclease (DNase I) in the detection cell can cleave the free aptamer (Hogan et al., 1989), thereby liberating the kanamycin molecules. The released target then hybridizes with a new aptamer on the electrode surface and initiates a new cycle of cleavage, leading to a target molecule recycling process, which leads to significant amplification of the signal. By monitoring the real-time change of the recorded potential in the smartphone, we could detect the target more sensitive and more convenient.

To testify the validity of the nuclease-assisted signal amplification potentiometric aptasensor, the EIS was applied to characterize the interfacial electrochemical information of paper electrodes in the presence and absence of aptamer, kanamycin molecule, and DNase I. EIS is an effective way to characterize the electron transfer performance of the electrodes after a series of modification and reaction. For the Nyquist plot, the semicircle part at higher frequencies represents the electron transfer process, and the linear part at lower frequencies reflects the diffusion process, and the semicircle diameter is equal to the electron/charge transfer resistance (R_{et}/R_{ct}) of electrode (Chang and Park, 2010). As illustrated in Fig. 2, it is demonstrated that the bare GNPE possesses a relatively minimum interfacial electron transfer resistance. With the modification of kanamycin aptamer, the electron transfer resistance of the obtained GNPE/aptamer was significantly increased compare the bare one, which was induced by the impeded electron transferring paths, confirming the successful modification of the biomolecules. As for the reaction process, the electron transfer resistance (R_{et}) of GNPE/aptamer was decreased after incubating in buffer solution containing kanamycin, since the kanamycin molecules bind with the aptamers specifically and then the aptamer/kanamycin conjugates release from the electrode surface restoring the paths of electron transferring. Furthermore, with the digestion of the DNase I, the aptamers of dissociative aptamer/kanamycin conjugates are cleaved and the released kanamycin molecules start a new cycle. As expected, the electron transfer resistance (R_{et}) of electrode decreases which demonstrates the reduced aptamers amounts on the surface of electrode under the nuclease-assisted amplified reaction. These results clearly suggest that the employment of DNase I could further improve the detection sensitivity of flexible potentiometric aptasensor.

3.2. Characterization of the paper electrodes

Freestanding GNP was fabricated from the graphene aqueous solution by vacuum filtration. As shown in Fig. 1**A and B**, the as-prepared GNP possesses a smooth surface and the fabricated GNP strip is very flexible. Scanning electron microscopy (SEM) was applied to observe the plane and entire cross-section morphology of GNP, respectively (Fig. 1**D and E**). The surface morphology of GNP exhibits many rolling wrinkles on account of the flexible nature of graphene nanosheets, a layer-by-layer ordered structure was observed in our prepared GNP, indicating a sheet-by-sheet self-assemble fashion occurs during the filtration process, resulting from the π-π stacking interaction between the graphene nanosheets. And the GNP used in this research possess a thickness of nearly 10 μm.

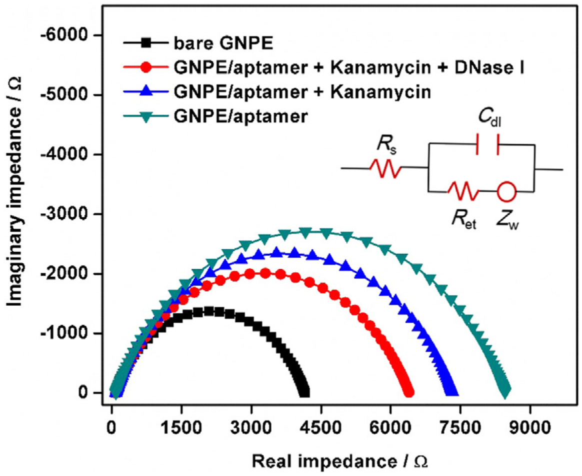

Fig. 2. Impedance spectra of bare GNPE, GNPE/aptamer, GNPE/aptamer after addition of kanamycin, and GNPE/aptamer after addition of kanamycin and DNase I in 0.1 M KCl aqueous solution containing 5.0 mM $K_3[Fe(CN)_6]/K_4[Fe(CN)_6]$ (1:1). DC potential: 0 mV, AC amplitude: 50 mV, scan frequency: 0.1 Hz–100 kHz (the inset is equivalent circuit).

Raman spectra was performed to determine the crystal structure of GNP. As shown in Fig. 1**C**, GNP is characteristic of two prominent peaks at 1352 and 1594 cm^{-1}, corresponding to the well-documented D and G bands, respectively. Furthermore, the intensity ratio of the two peaks (I_D/I_G) of GNP (1.59) increased in comparison with that of the GOP (0.98), confirming that ordered structure is partially restored in rGO sheets after the chemical reduction by ascorbic acid. The electrochemical characteristics of bare GCE and the prepared GNPE are explored by choosing the $[Fe(CN)_6]^{3-/4-}$ as redox probe in 0.1 M KCl solution at a scan rate of 100 mV/s. As reflected by CV curves shown in Fig. 1**F**, a pair of quasi-reversible Faradic currents associated with the well-defined redox waves of the $[Fe(CN)_6]^{3-/4-}$ couple were presented in both of the GCE and GNPE, however, the Faradic current and the capacitive current of GNPE are larger than bare GCE, demonstrating the accelerated electron transfer kinetics resulting from the increased specific surface area and double layer capacitance of GNPE.

3.3. Analytical performance of potentiometric aptasensor

The fabricated potentiometric aptasensor was used for the quantification of kanamycin molecules by adding different concentrations of the target into the detection cell. First of all, the bare GNPE and GNPE/aptamer without the assistance of DNase I were tested for comparison purposes. Consecutive additions of increased amounts of kanamycin from 0.02 ng/mL to 150 ng/mL in Tris-buffer solution (20 mM, pH 7.4) were performed to test the response of these paper sensor, which was recorded in a Smartphone. As shown in Fig. 3**A**, negligible potentiometric response of the bare GNPE with the increasing concentration of the target could be observed. The potentiometric response of GNPE/aptamer without DNase I was also presented, the recorded EMF value started to increase until the kanamycin concentration was up to 50 ng/mL, indicating that the signal was produced by the recognition of the

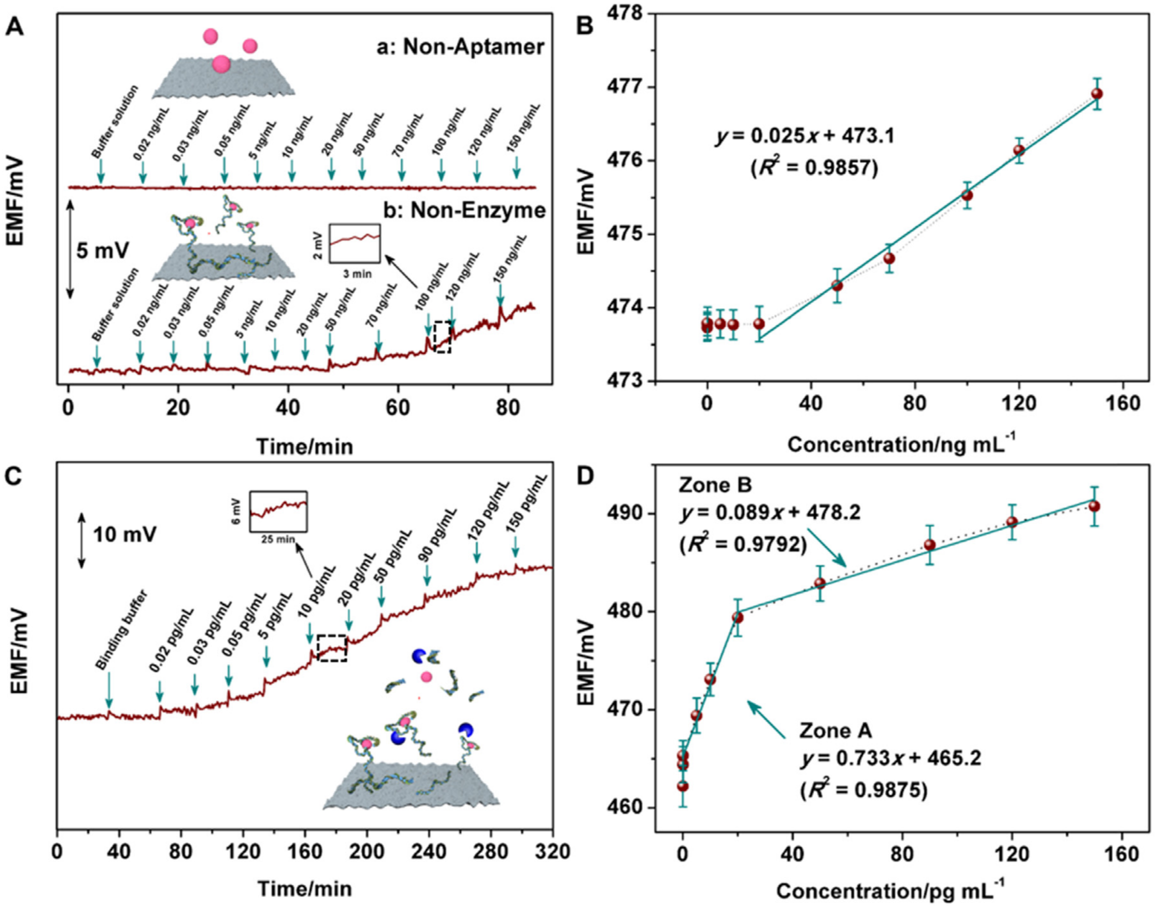

Fig. 3. (A, B) Potentiometric response of bare GNPE and GNPE/aptamer without the addition of DNase I exposed to stepwise increases of kanamycin (A) and the corresponding calibration curves of GNPE/aptamer (B). Inset of (A) is the enlargement of the selected area. (C, D) Potentiometric response of GNPE/aptamer with the addition of DNase I exposed to stepwise increases of kanamycin (C) and the corresponding calibration curves (D) (the arrows represent the inoculations with targets and values are the final concentration). Inset of (C) is the enlargement of the selected area.

target by the aptamer modified on the electrode. A linear range from 50 ng/mL to 150 ng/mL (R^2 = 0.9857) could be obtained from the corresponding calibration curve (Fig. 3**B**). The small molecule of kanamycin causes small EMF value changes under the 1:1 binding strategy without amplification process which make the detection method exhibits low sensitivity.

To amplify the signal response of the fabricated potentiometric aptasensor, we applied a convenient catalytic recycling strategy based on the adoption of DNase I, which was testified on a graphene-based fluorescent aptasensor for the detection of small molecular before (Lu et al., 2010). Here, we used the DNase I as unmodified nuclease in detection cell to cleavage the dissociative aptamer and release kanamycin into the binding reaction cycle again. Fig. 3**C** presents the EMF value of the GNPE/aptamer-based potentiometric aptasensor exposed to the increased kanamycin from 0.02 pg/mL to 150 pg/mL with the assistance of DNase I (10 unit). A stable EMF response could be reached after 25–30 min (inset of Fig. 3**C**), to ensure the accurate measurement of the potentiometric response, the kanamycin was stepwise added to the detection cell for every 30 min. In contrast to the 1:1 binding strategy, a dramatic increase of the potentiometric value could be obtained. From the EMF response of the GNPE/aptamer electrode without kanamycin molecule but exposed to DNase I (10 units) shown in Fig. S1 (Supporting information), it can be seen that no obvious potential drift after the addition of DNase I, confirming that kanamycin aptamer was solidly adsorbed on the surface of GNPE in the detection environment, which was further testified that the EMF responses exhibited in Fig. 3**C** were caused by kanamycin molecules. The response in the whole concentration range presented two obviously different zones termed zone A and B. A steep slope (recorded as 0.733) was acquired at the concentration of kanamycin lower than 20 pg/mL (zone A), probably due to the high affinity interaction between the aptamer and the target molecules. With the concentration of kanamycin above the 20 pg/mL, the potentiometric response was less received (zone B) with a slope value as low as 0.089, presumably demonstrating the drastic reduction of the aptamer amounts on the electrode surface after a series of circular reaction (Fig. 3**D**). To simplify the relevance, both regions can be fitted into a linear model, the linear range could be divided as 0.03–20 pg/mL (R^2 = 0.9875) and 20–150 pg/mL (R^2 = 0.9792), the detection limit (defined for classical potentiometric sensors as the intersection of the two straight lines) of kanamycin acquired from zone A was 0.03 pg/mL (i.e. 0.05 pM). Furthermore, the analytical performance towards kanamycin detection of the fabricated aptasensor and other sensors reported previously was summarized in Table 1 for a comparison. It is clear to see that although the system has not yet been optimized for maximum efficacy, the sensitivity of our potentiometric enzymatic aptasensor assay for the detection of kanamycin was more than several orders of magnitude higher than that of other reported assays.

3.4. Selectivity of the potentiometric enzymatic aptasensor

Selectivity is another important criterion of the fabricated aptasensor for the detection of kanamycin. To testify this property, we applied the detection system for four antibiotics of kanamycin analogues with the same concentration (20 pg/mL), including amoxicillin, ciprofloxacin, tetracycline, and chloramphenicol. As illustrated in Fig. 4**A**,

Table 1
Comparison of the performance of our developed potentiometric aptasensor with other reported kanamycin sensors.

Analytical method	Immobilized receptor	Concentration range	Detection limit	References
ELISA	Antibody	0.34–86 nM	0.34 nM	(Melville et al., 1999)
SPR	Au NPs	1.0–1000 pM	1.0 pM	(Frasconi et al., 2010)
HPLC	–	10–150 nM	25 nM	(Blanchaert et al., 2013)
Colorimetric method	Aptamer	0.43–3.43 mM	65 μM	(Song et al., 2011)
Luminescent method	Aptamer	0.5–20 nM	321 pM	(Ramezani et al., 2016)
DPV	Aptamer	0.02–258 nM	8.6 pM	(Song et al., 2016)
Potentiometry	Aptamer	0.05–30 pM[a]	0.05 pM[a]	This work

Abbreviation. ELISA: enzyme-linked immunosorbent assay. SPR: surface plasmon resonance. HPLC: high-performance liquid chromatography. DPV: differential pulse voltammetry.

[a] : 0.05–0.3 pM is worked out via dividing 0.03–20 pg/mL by the molecular weight of kanamycin sulfate (582.58 g/mol).

significant EMF response was recorded with the kanamycin compared to those obtained from other antibiotics. These results demonstrate that the high specificity of our GNPE/aptamer-based potentiometric enzymatic aptasensor for kanamycin detection, which could be contributed to the specific recognition of aptamer towards the target molecular kanamycin.

3.5. *Flexibility of the potentiometric enzymatic aptasensor*

The high flexibility of paper-like electrode is one of the determining factor of the operation stability for advanced implantable biomedical devices and miniaturized lap-on-a-chip devices when applying in the assay of real samples. Therefore, we tested the influence of mechanical stress induced by the continuous bending on the overall signal output performance of GNPE/aptamer-based potentiometric aptasensors. As shown in Fig. 4**B**, after bending with various times at different angles, the EMF drifts of the GNPE/aptamer-based aptasensors recorded from 4 h continuous monitoring were less than 1.1%. The relative standard deviation (RSD) value of relative response for 30°, 60°, and 90° bending was 0.92%, 0.98%, and 1.07%, respectively. Such a negligible influence of mechanical stress on the EMF response indicates that our developed potentiometric enzymatic aptasensor possesses excellent flexibility, which could be further incorporated into accurate micro-integrated detection system for biochemical applications.

3.6. *Stability and reproductivity of the potentiometric enzymatic aptasensor*

The storage stability of the freestanding GNPE/aptamer electrode in potentiometric detection was tested, to be specific, the EMF response of the same electrode in buffer solution containing DNase I was periodically recorded. As shown in Fig. S2A (Supporting information), the potentiometric aptasensor yields a RSD of 3.98%, and retained 98.6% of its initial EMF value after nine days interval measuring. Therefore, the freestanding GNPE/aptamer electrodes possess comparable stability for a long-term storage. The reproducibility of the freestanding GNPE/aptamer electrode for kanamycin detection was also examined, the EMF measurement was carried out on ten GNPE/aptamer electrodes which were exposed to 50 pg/mL kanamycin. From the variation of EMF value presented in Fig. S2B (Supporting information), the RSD of the tested electrodes was founded to be 1.73%, which demonstrates that the developed potentiometric enzymatic aptasensor possesses an excellent reproducibility for the determination of kanamycin.

3.7. *Real analysis for milk samples*

To testify the feasibility of the fabricated potentiometric enzymatic aptasensors, the recovery test were performed in real samples which were spiked with a certain concentration of kanamycin. Milk, as the most widely consumed food product all over the world, was selected for sample analysis detection. It is of great significance for human health to detect kanamycin residue in milk. Five kanamycin-free milk samples purchased from local supermarket were added with 50 pg/mL kanamycin for recovery test. The recovery values of kanamycin presented in Table S1 (Supporting information) are between 104.66% and 115.72% with a RSD range from 3.94% to 4.32% are obtained. All these demonstrate that the fabricated potentiometric aptasensor is reliable for kanamycin residues detection in real samples.

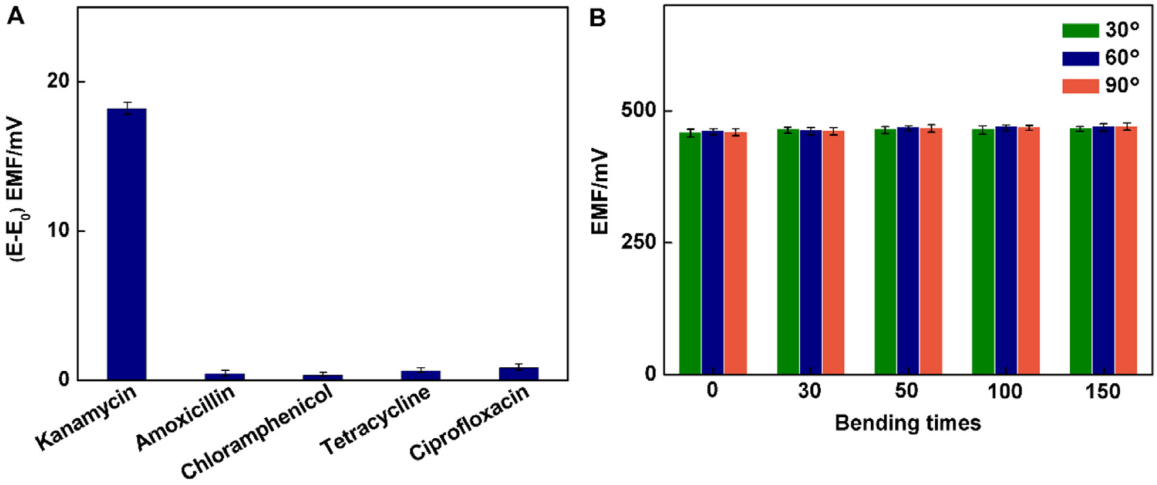

Fig. 4. (A) Selectivity of the GNPE/aptamer-based potentiometric aptasensor for the detection of kanamycin. The tested concentration of kanamycin and four antibiotics of kanamycin analogues (amoxicillin, ciprofloxacin, tetracycline, and chloramphenicol) was 20 pg/mL. (B) Effects of bending angles and bending times on stability of GNPE/aptamer-based potentiometric aptasensors.

4. Conclusions

In this work, ultrasensitive wireless detection of kanamycin was realized using a flexible potentiometric enzymatic aptasensor combined with a smartphone. With the introduction of nuclease, a catalytic cycling binding reaction between free kanamycin and immobilized aptamer occurred. As expected, an ultra-low detection limit of 30.0 fg/mL for kanamycin was obtained. And the developed potentiometric enzymatic aptasensor exhibits high selectivity, favorable flexibility, excellent stability and reproducibility. Moreover, the prepared aptasensor was used for kanamycin detection in milk samples with satisfactory results. This work paves a useful way for implementation of free-standing paper-like graphene-based macroscopic materials and enzyme-based amplification detection strategy into potentiometric biosensors, which could significantly expand the scope of potentiometric sensing devices and holds great application prospects in micro-integrated detection system for human health.

Acknowledgements

This research was supported by the National Natural Science Foundation of China (No. 31301468).

Appendix A. Supplementary material

Supplementary data associated with this article can be found in the online version at doi:10.1016/j.bios.2018.08.048.

References

Acerce, M., Akdoğan, E.K., Chhowalla, M., 2017. Nature 549, 370–373.
Bai, X., Hou, H., Zhang, B., Tang, J., 2014. Biosens. Bioelectron. 56, 112–116.
Bakker, E., Pretsch, E., 2007. Angew. Chem. Int. Ed. 46, 5660–5668.
Ballard, D.G.H., Rideal, G.R., 1983. J. Mater. Sci. 18, 545–561.
Blanchaert, B., Jorge, E.P., Jankovics, P., Adams, E., Schepdael, A.V., 2013. Chromatographia 76, 1505–1512.
Chang, B.Y., Park, S.M., 2010. Annu. Rev. Anal. Chem. 3, 207–229.
Chem, A., 2012. Anal. Chem. 84, 4695–4702.
Chen, J., Li, Z., Ge, J., Yang, R., Zhang, L., Qu, L.B., Wang, H.Q., Zhang, L., 2015. Talanta 139, 226–232.
Chen, S.H., Liang, Y.C., Chou, Y.W., 2006. J. Sep. Sci. 29, 607–612.
Cong, H.P., Ren, X.C., Wang, P., Yu, S.H., 2013. Energy Environ. Sci. 6, 1185–1191.
Ellington, A.D., Szostak, J.W., 1992. Nature 355, 850–852.
Frasconi, M., Telvered, R., Riskin, M., Willner, I., 2010. Anal. Chem. 82, 2512–2519.
Gaudin, V., Cadieu, N., Maris, P., 2003. Food Agric. Immunol. 15, 143–157.
Guo, C.X., Ng, S.R., Khoo, S.Y., Zheng, X., Chen, P., Li, C.M., 2012. ACS Nano 6, 6944–6951.
Guo, W., Sun, N., Qin, X., Pei, M., Wang, L., 2015. Biosens. Bioelectron. 74, 691–697.
Gwon, H., Kim, H.S., Lee, K.U., Seo, D.H., Yun, C.P., Lee, Y.S., Ahn, B.T., Kang, K., 2011. Energy Environ. Sci. 4, 1277–1283.
Hernández, R., Vallés, C., Benito, A.M., Maser, W.K., Rius, F.X., Riu, J., 2014. Biosens. Bioelectron. 54, 553–557.
Hogan, M.E., Roberson, M.W., Austin, R.H., 1989. Proc. Natl. Acad. Sci. USA 86, 9273–9277.
Hu, L., Xu, G., 2010. Chem. Soc. Rev. 39, 3275–3304.
Jr, W.S.H., Offeman, R.E., 1958. J. Am. Chem. Soc. 80, 1339.
Kaale, E., Van, S.A., Roets, E., Hoogmartens, J., 2001. J. Chromatogr. A 924, 451–458.
Kovtyukhova, Nina I., Ollivier, Patricia J., Martin, Benjamin R., Chizhik, Sergey A., Buzaneva, Eugenia V., Gorchinskiy, A.D., 1999. Chem. Mater. 11, 771–778.
Lan, L., Yao, Y., Ping, J., Ying, Y., 2017. Biosens. Bioelectron. 91, 504–514.
Liu, J., Cao, Z., Lu, Y., 2009. Chem. Rev. 109, 1948–1998.
Lu, C.H., Li, J., Lin, M.H., Wang, Y.W., Yang, H.H., Chen, X., Chen, G.N., 2010. Angew. Chem. Int. Ed. 49, 8454–8457.
Manyanga, V., Dhulipalla, R.L., Hoogmartens, J., Adams, E., 2010. J. Chromatogr. A 1217, 3748–3753.
Mayer, G., 2010. Angew. Chem. Int. Ed. 121, 2710–2727.
Melville, P.A., Watanabe, E.T., Benites, N.R., Ribeiro, A.R., Silva, J.A.B., Jr, F.G., Costa, E.O., 1999. Mycopathologia 146, 79–82.
Park, S., An, J., Suk, J.W., Ruoff, R.S., 2010. Small 6, 210–212.
Ping, J., Wang, Y., Fan, K., Wu, J., Ying, Y., 2011. Biosens. Bioelectron. 28, 204–209.
Ping, J., Wang, Y., Fan, K., Tang, W., Wu, J., Ying, Y., 2013. J. Mater. Chem. B 1, 4781–4791.
Ping, J., Zhou, Y., Wu, Y., Papper, V., Boujday, S., Marks, R.S., Steele, T.W., 2015. Biosens. Bioelectron. 64, 373–385.
Pitkethly, M.J., 2004. Mater. Today 7, 20–29.
Prosen, C.A., Petersen, M.R., Moody, D.B., Stebbins, W.C., 1978. J. Acoust. Soc. Am. 63, 559–566.
Ramezani, M., Danesh, N.M., Lavaee, P., Abnous, K., Taghdisi, S.M., 2016. Sens. Actuators B 222, 1–7.
Samsonova, Z.V., Shchelokova, O.S., Ivanova, N.L., Rubtsova, M.Y., Egorov, A.M., 2005. Appl. Biochem. Microbiol. 41, 589–595.
Sentic, M., Arbault, S., Bouffier, L., Manojlovic, D., Kuhn, A., Sojic, N., 2015. Chem. Sci. 6, 4433–4437.
Song, H.Y., Kang, T.F., Li, N.N., Lu, L.P., Cheng, S.Y., 2016. Anal. Methods 8, 3366–3372.
Song, K.M., Cho, M., Jo, H., Min, K., Jeon, S.H., Kim, T., Han, M.S., Ku, J.K., Ban, C., 2011. Anal. Biochem. 415, 175–181.
Spahn, C.M.T., Prescott, C.D., 1996. J. Mol. Med. 74, 423–439.
Tachibana, M., Mizukoshi, O., Kuriyama, K., 1976. Biochem. Pharmacol. 25, 2297–2301.
Tuerk, C., Gold, L., 1990. Science 249, 505–510.
Varghese, N., Mogera, U., Govindaraj, A., Das, A., Maiti, P.K., Sood, A.K., Rao, C.N., 2010. ChemPhysChem 10, 206–210.
Wan, Y.J., Zhu, P.L., Yu, S.H., Sun, R., Wong, C.P., Liao, W.H., 2017. Carbon 122, 74–81.
Wang, Y., Ping, J., Ye, Z., Wu, J., Ying, Y., 2013. Biosens. Bioelectron. 49, 492–498.
Willner, I., Zayats, M., 2007. Angew. Chem. Int. Ed. 119, 6528–6538.
Wirmer, J., Westhof, E., 2006. Methods Enzymol. 415, 180–202.
Xiao, F., Li, Y., Zan, X., Liao, K., Xu, R., Duan, H., 2012. Adv. Funct. Mater. 22, 2487–2494.
Xu, Y., Han, T., Li, X., Sun, L., Zhang, Y., Zhang, Y., 2015. Anal. Chim. Acta 891, 298–303.
Yao, Y., Ping, J., 2018. TrAC-Trend Anal. Chem. 105, 75–88.
Yu, C.Z., He, Y.Z., Fu, G.N., Xie, H.Y., Gan, W.E., 2009. J. Chromatogr. B 877, 333–338.
Zan, X., Bai, H., Wang, C., Zhao, F., Duan, H., 2016. Chemistry 22, 5204–5210.
Zelada-Guillén, G.A., Riu, J., Düzgün, A., Rius, F.X., 2009. Angew. Chem. Int. Ed. 48, 7334–7337.
Zhang, F., Yuan, C., Zhu, J., Wang, J., Zhang, X., Lou, X.W., 2013. Adv. Funct. Mater. 23 (3944-3944).
Zhang, J., Yang, H., Shen, G., Cheng, P., Zhang, J., Guo, S., 2010. Chem. Commun. 46, 1112–1114.